Diffuse interfaces and transformation fronts modelling in compressible media

Richard Saurel and Fabien Petitpas

Aix Marseille University, IUSTI UMR CNRS 7343, 5 rue E. Fermi, 13453 Marseille, France
also, RS2N, Bastidon de la Caou, 13360 Roquevaire, France

Abstract

Multi-material computations have to deal with mixture cells with interfaces separating fluids, phases or materials in the same control volume or computational cell. The difficulty is to compute the correct thermodynamic and kinematic state while ensuring the correct jump/coupling conditions. Two mains class of methods are available to do this. The first one considers interfaces as sharp discontinuities. Lagrangian, Front Tracking and Interface Reconstruction methods belong to this class. The second option consists in the building of a flow model valid everywhere, in pure materials and mixture cells, solved routinely with a unique Eulerian algorithm (Saurel and Abgrall, 1999). In this frame, the interface is considered as a numerically diffused zone, captured by the algorithm. There are some advantages with this approach, as the corresponding 'diffuse interface' flow models are not valid in mixture cells only as they also describe accurately true multiphase mixtures of materials.
This approach was reduced by Kapila et al. (2001) with the help of asymptotic analysis, resulting in a single velocity, single pressure but multi-temperature flow model. This model present serious difficulties for its numerical resolution as one of the equations is non-conservative, but is an excellent candidate to solve mixture cells as well as pure fluids. In the presence of shocks, jump conditions have to be provided. They have been determined in Saurel et al. (2007) in the weak shock limit. When compared against experiments for both weak and strong shocks, excellent agreement was observed. These relations are accepted as closure relations for the Kapila et al. (2001) model in the presence of shocks. Capillary effects (Perigaud and Saurel, 2005) as well as phase transition modelling have been addressed too (Saurel et al., 2008). With this extension it is possible to deal with high speed cavitating and flashing flows. Oppositely to the previous examples of endothermic phase transition, when exothermic effects are considered as for example with high energetic materials, detonation waves appear. With the help of the shock relations and governing equations inside the reaction zone, generalized Chapman-Jouguet conditions are obtained as well as heterogenous explosives detonation wave structure (Petitpas et al., 2009). Extra multiphysic extensions such as dynamic powder compaction (Saurel et al., 2010), solid-fluid coupling in extreme deformations (Favrie et al., 2009) are possible too.

Key words: hyperbolic systems, interfaces, multiphase flows, detonations, cavitation

1 Introduction

The computation of interfaces and waves dynamics with compressible materials has many fundamental and industrial applications, ranging from fluid mechanics and astrophysics to chemical, mechanical and environmental engineering. When dealing with compressible materials the main issue is related to the appearance of mixture cells. These mixture cells are consequences of fluid motion and artificial smearing of discontinuities. The correct computation of the entire flow field requires perfect fulfilment of the interface conditions. In the simplest situation of contact interfaces with perfect fluids, these conditions correspond to equal normal velocities and equal pressures. To compute compressible flows with interfaces two main class of approaches are available. In the first one, the interface is considered as a sharp discontinuity. To avoid as far as possible interface numerical smearing several options are possible:
- Lagrangian and ALE methods (see for example Hirt et al., 1974, Farhat and Roux, 1991). In this

context, the computational mesh moves and distorts with the material interface. However, when dealing with fluid flows, deformations are unbounded and resulting mesh distortions may result in computational failure (Scheffer and Zukas, 2000).
- Interface Reconstruction methods use a fixed mesh with an additional equation for tracking or reconstructing the material interface. In the volume of fluid (VOF) approach (Hirt and Nichols, 1981), each computational cell is assumed to possibly contain a mixture of fluids and the volume occupied by each fluid is represented by the volume fraction, transported with the flow. This method is widely used for incompressible flows as there is no thermodynamics to compute in mixture cells (Gueyffier et al., 1999). For compressible flows, extra energy equations are used as well as pressure relaxation procedures (Benson, 1992, Miller and Puckett, 1996). Multiphase flow ingredients are used with these methods that come quite close to the diffuse interface methods discussed later.
- Level-Set methods (Mulder et al., 1992, Osher and Fedkiw, 2001, Sethian, 2001) are very popular methods to spatially locate interfaces. Special management of the interfaces is needed to preserve jump conditions. Relevant work in this direction was done by Fedkiw et al. (1999) with the Ghost Fluid Method.
- Front Tracking methods consider explicit interface tracking over a fixed Eulerian mesh (LeVeque and Shyue, 1996, Glimm et al., 1998).
With the various preceding methods, the interface is managed with a specific treatment, having consequences with respect to coding complexity, conservation issues, extra physics extension capabilities and robustness especially in severe conditions.
The second class of approaches follows another philosophy, closer to the one of capturing methods. Capturing methods are fundamental contributions of Von Neumann and Richtmyer (1950) and Godunov (1959). The aim was to solve the same equations with the same numerical scheme in both smooth and discontinuous flow regions. Pioneer works in 'interface capturing' or 'diffuse interface' modelling areas were done about forty years latter by Karni (1994). Indeed, interfaces computation posed extra difficulties linked to thermodynamic state computation in artificial mixture zones.
Determination of thermodynamic flow variables in these mixture zones has been achieved on the basis of multiphase flow modelling by Saurel and Abgrall (1999). Some advantages appeared:
- As already mentioned, the same equations were solved everywhere (interfaces, shocks, expansions waves) with a unique flow solver.
- These models and methods were able to dynamically create interfaces (not present initially) as for example in cavitating flows (Saurel and Le Metayer, 2001, Saurel et al., 2008).
- These methods were also able to deal with interfaces separating pure fluids and fluid mixtures, as for example when a granular material is in contact with a fluid (Chinnayya et al., 2004, Saurel et al., 2010).
- As this approach includes the two velocities flow model of Baer and Nunziato (1986) it is also possible to compute velocity non-equilibrium bubbly or granular flows in conjunction with material interfaces (Gavrilyuk and Saurel, 2002, Saurel et al., 2003).
In the same period of time, reduced models have been built by Kapila et al. (2001). Here, pressure and velocity equilibrium is assumed, rendering the resulting model unable to deal with velocity non-equilibrium mixtures, but resulting in a more appropriate model for interface computations.
As it is more convenient to add extra physics in a single velocity context, multiphysics capabilities have been considered in the Kapila et al. (2001) frame. Surface tension modelling (Perigaud and Saurel, 2005), shock and detonation computation in heterogeneous materials (Saurel et al., 2007, Petitpas et al., 2009), phase transition (Saurel et al., 2008), elastic solid - fluid coupling (Favrie et al., 2009), powder compaction (Saurel et al., 2010), interpenetration effects at unstable interfaces (Saurel et al., 2012) are examples of such extensions.
To summarize, diffuse interface modelling allows quite advanced multiphysics extensions still solving a unique set of hyperbolic partial differential equations with a unique Godunov type flow solver.
The aim of the present paper is not to summarize all these possible extensions but to give a comprehensive introduction to the 'diffuse interface' approach. To do this, Section 2 presents a hyperbolic non-equilibrium two-phase model that is a good starting point to describe natural or artificial two-phase mixtures. The Kapila et al. (2001) model is presented in Section 3 as a reduced version of the previous non-equilibrium model. This model is the simplest candidate for diffuse interface modelling with non-barotropic fluids. The Kapila et al. (2001) model being non conservative, shock relations have to be determined as well as appropriate numerical schemes. The Saurel et al.

(2007) shock relations are presented in the same section and the relaxation algorithm of Saurel et al. (2009) is summarized in Section 4. Some extensions are presented in Section 5 with capillary effects. Phase transition modelling is addressed in Section 6 and detonation modelling is addressed in Section 7. Section 8 deals with open issues, such as low Mach number flows with diffuse interface models, diffuse interfaces sharpening and extra multiphysics extensions.

2 Total disequilibrium mixtures

The Kapila et al. (2001) model we are going to use for the various multiphysics extensions comes from a more general model, out of mechanical, thermal and chemical equilibrium. The non-equilibrium mixture model presented hereafter consists in a symmetric formulation of the Baer and Nunziato (1986) model developed in Saurel et al. (2003):

$$\begin{aligned}
&\frac{\partial \alpha_1}{\partial t} + u_I \frac{\partial \alpha_1}{\partial x} = \mu(p_1 - p_2), \\
&\frac{\partial (\alpha\rho)_1}{\partial t} + \frac{\partial (\alpha\rho u)_1}{\partial x} = 0, \\
&\frac{\partial (\alpha\rho u)_1}{\partial t} + \frac{\partial (\alpha\rho u^2 + \alpha p)_1}{\partial x} = p_I \frac{\partial \alpha_1}{\partial x} - \lambda(u_1 - u_2), \\
&\frac{\partial (\alpha\rho E)_1}{\partial t} + \frac{\partial (\alpha(\rho E + p)u)_1}{\partial x} = p_I u_I \frac{\partial \alpha_1}{\partial x} - \lambda u_I'(u_1 - u_2) - \mu p_I'(p_1 - p_2).
\end{aligned} \tag{2.1}$$

The second phase obeys a symmetrical set of equations. This model is hyperbolic and fulfils the second law of thermodynamics. The closure relations for the relaxation parameters (μ and λ) as well as for interfacial variables estimates u_I, u_I', p_I, p_I' are given in the same reference.

This model is able to describe two-phase mixtures out of velocity equilibrium. Wave's propagation is preserved thanks to the hyperbolic character of the equations and to the presence of relaxation effects.

This model can be used for the computation of interface problems with perfect fulfilment of interface conditions. This goal can be reached with two different options:

- The first option consists in using stiff mechanical relaxation parameters μ and λ (Saurel and Abgrall, 1999).

- The second one is based on non-conservative terms $u_I \frac{\partial \alpha_1}{\partial x}$, $p_I \frac{\partial \alpha_1}{\partial x}$ (Abgrall and Saurel, 2003).

The first method is simple and robust. The second one is more subtle but renders possible the consideration of zones out of velocity equilibrium in conjunction with macroscopic interfaces where normal velocity and pressures have to be equal. In particular, it is able to deal with bubble cloud crossing through material interfaces.

Consideration of extra physics is this formulation is possible but easier in the frame of single velocity formulations. The rest of this paper places in this context, as single velocity models are suitable for many applications.

3 Mechanical equilibrium model – Diffuse interfaces

The Kapila et al. (2001) model is obtained as asymptotic limit at zero order of the previous model in the limit of relaxation parameters μ and λ tending to infinity. Therefore it corresponds to the first option mentioned previously with the non-equilibrium model. It reads:

$$\begin{aligned}
&\frac{\partial \alpha_1}{\partial t} + u \frac{\partial \alpha_1}{\partial x} = \alpha_1 \alpha_2 \frac{\rho c_W^2}{\rho_1 c_1^2 \rho_2 c_2^2} \left(\rho_2 c_2^2 - \rho_1 c_1^2\right) \frac{\partial u}{\partial x}, \\
&\frac{\partial (\alpha\rho)_1}{\partial t} + \frac{\partial (\alpha\rho)_1 u}{\partial x} = 0, \\
&\frac{\partial (\alpha\rho)_2}{\partial t} + \frac{\partial (\alpha\rho)_2 u}{\partial x} = 0,
\end{aligned} \tag{3.1}$$

$$\frac{\partial \rho u}{\partial t} + \frac{\partial \left(\rho u^2 + p\right)}{\partial x} = 0,$$
$$\frac{\partial \rho E}{\partial t} + \frac{\partial \left((\rho E + p)u\right)}{\partial x} = 0.$$

The total energy is defined as $E = Y_1 e_1 + Y_2 e_2 + \frac{1}{2}u^2$ where $Y_k = \frac{(\alpha\rho)_k}{\rho}$ represent the mass fractions and $\rho = \sum_k (\alpha\rho)_k$ the mixture density. This model is hyperbolic too with the same wave speeds as the gas dynamic equations but with the Wood (1930) sound speed, that presents a non monotonic behaviour with respect to the volume fraction: $\frac{1}{\rho c_w^2} = \sum_k \frac{\alpha_k}{\rho_k c_k^2}$. The equation of state allowing the thermodynamic closure is obtained from the mixture energy definition and the pressure equilibrium condition. This equation of state involves at least three arguments: $p = p(\rho, e, \alpha_1)$. For example, when each phase obeys the stiffened gas equation of state (see Le Metayer et al., 2004 for parameters determination),

$$p_k = (\gamma_k - 1)\rho_k e_k - \gamma_k p_{\infty k}, \tag{3.2}$$

the mixture equation of state then reads,

$$p(\alpha_k, \rho_k, e) = \frac{\rho e - \sum_k \frac{\alpha_k \gamma_k p_{\infty k}}{\gamma_k - 1}}{\sum_k \frac{\alpha_k}{\gamma_k - 1}} \quad . \tag{3.3}$$

Parameters γ_k and $p_{\infty k}$ are characteristic constants of material k. As this model involves a single pressure but two mass equations and a volume fraction equation, it is possible to determine two temperatures ($T_k = T_k(p, \rho_k)$) and two entropies. This feature will be useful for phase transition modelling.

This model is an excellent candidate for interface problem computations. However, two difficulties at least are present:

- Conventional Rankine-Hugoniot cannot be determined in a conventional way as the volume fraction equation is non-conservative. With other sets of variables, it is no more possible to obtain meaningful jump conditions.

- The numerical resolution of this model is intricate, due to the presence of the same equation.

The first issue has been considered in Saurel et al. (2007). Shock jump conditions have been determined in the weak shock limit. When compared against experimental data of shock speeds in mixtures of materials, for shocks of arbitrary strength (in the megabar range), excellent agreement was obtained. All available data in the Russian and American databases have been used in this aim. The corresponding algebraic system reads:

$$\left[(\alpha\rho)_k (u - \sigma)\right] = 0, \text{ k=1,2,}$$
$$\left[\rho u(u - \sigma) + p\right] = 0, \tag{3.4}$$
$$e_k - e_{k0} + \frac{p + p_0}{2}(v_k - v_{k0}) = 0, \text{ k=1,2.}$$

A comparison example is given in the Figure 1 for a representative mixture of materials, made of epoxy and spinel. Mixture composition and equations of state parameters are given in Saurel et al. (2007).

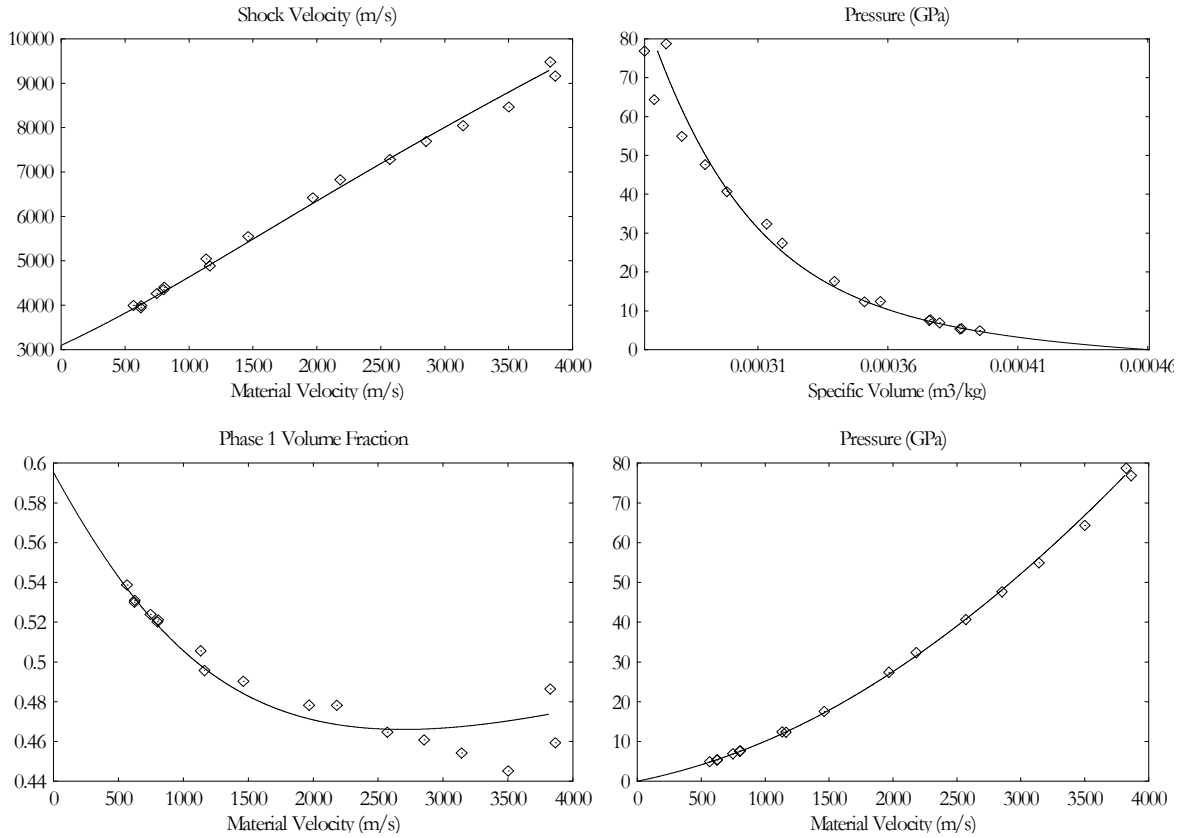

Figure 1. Comparison between experiments (symbols) and results obtained from Rankine-Hugoniot relations (3.4) for the Epoxy-Spinel mixture. Excellent agreement is observed. The same agreement is observed for all mixtures free of phase transition having experimental data in the Russian and American databases.

The second difficulty, related to the numerical approximation of System (3.1) has been addressed in Saurel et al. (2009) with the strategy summarized in the next section.

4 Simple and efficient relaxation method

To solve System (3.1), an extended system is considered, that seems more complex at a first glance. However, with this extended system, there is no difficulty to preserve volume fraction positivity. Also, the sound speed with the new model is monotonic with respect to the volume fraction. Last, the Riemann problem resolution is straightforward as will be shown later, as the volume fraction has no jumps across the right and left facing waves.

Nevertheless, to recover solutions of the mechanical equilibrium model (3.1), stiff pressure relaxation has to be used, preserving also volume fraction positivity.

Therefore, the model is solved in a sequence of three steps:

- Solve the extended pressure non-equilibrium flow model with appropriate hyperbolic solver.

- Relax the pressure toward mechanical equilibrium.

- Reset the internal energies with the help of the mixture equation of state (3.3).

Each step is summarized hereafter.

The pressure non-equilibrium model reads:

$$\frac{\partial \alpha_1}{\partial t} + u \frac{\partial \alpha_1}{\partial x} = \mu (p_1 - p_2)$$

$$\frac{\partial (\alpha\rho)_1}{\partial t} + \frac{\partial (\alpha\rho)_1 u}{\partial x} = 0,$$

$$\frac{\partial(\alpha\rho)_2}{\partial t}+\frac{\partial(\alpha\rho)_2 u}{\partial x}=0\,, \tag{4.1}$$

$$\frac{\partial \rho u}{\partial t}+\frac{\partial\left(\rho u^2+\alpha_1 p_1+\alpha_2 p_2\right)}{\partial x}=0$$

$$\frac{\partial \alpha_1\rho_1 e_1}{\partial t}+\frac{\partial \alpha_1\rho_1 e_1 u}{\partial x}+\alpha_1 p_1\frac{\partial u}{\partial x}=-p_I\mu(p_1-p_2)$$

$$\frac{\partial \alpha_2\rho_2 e_2}{\partial t}+\frac{\partial \alpha_2\rho_2 e_2 u}{\partial x}+\alpha_2 p_2\frac{\partial u}{\partial x}=p_I\mu(p_1-p_2)$$

Combination of the internal energy equations with mass and momentum equations results in the additional mixture energy equation:

$$\frac{\partial \rho\left(\sum_k Y_k e_k+\frac{1}{2}u^2\right)}{\partial t}+\frac{\partial\left(\rho\left(\sum_k Y_k e_k+\frac{1}{2}u^2\right)+\sum_k \alpha_k p_k\right)u}{\partial x}=0 \tag{4.2}$$

This extra equation is important during numerical resolution, in order to correct inaccuracies due to the numerical approximation of the non-conservative internal energy equations in the presence of shocks.

This model exhibits a nice feature regarding the mixture sound speed that reads,

$$c_f^2=\sum_k Y_k c_k^2\ ,$$

and has a monotonic behaviour versus volume and mass fractions. It represents the frozen mixture speed of sound with respect to the pressure relaxation effects. The model is thus hyperbolic with waves speeds: $u+c_f$, $u-c_f$, u .

System (4.1) is aimed to replace direct resolution of System (3.1) by the three steps method mentioned previously. During the first step, System (4.1) is solved in absence of relaxation terms $(\mu=0)$. Then relaxation terms are considered and are assumed stiff. In other word, the mechanical equilibrium solution is obtained at the end of the second step. It can be proved by asymptotic analysis that such strategy yields precisely to System (3.1) (see Saurel et al. 2009 Appendix B for the details).

Numerical resolution of the pressure non-equilibrium model in the limit of stiff pressure relaxation is then addressed. In regular zones, this model is self consistent. But in the presence of shocks the internal energy equations are inappropriate. To correct the thermodynamic state predicted by these equations in the presence of shocks, the total mixture energy equation is used. This correction is valid on both sides of the interface, when the flow tends to the single phase limits. The details of this correction will be examined further. For now, the pressure non-equilibrium system (4.1) is augmented by the redundant equation (4.2).

Hyperbolic solver

The hyperbolic solver is used to solve System (4.1-4.2) in the absence of relaxation terms $(\mu=0)$. The first ingredient corresponds to the Riemann solver used to compute the fluxes that cross each cell boundary. Then the variables are updated with a Godunov type method.

HLLC Riemann solver

The Toro et al. (1994) solver is considered at cell boundaries, separating left (L) and right (R) states. This solver involves 3 waves, is genuinely positive and valid for any convex equation of state. It is thus an excellent candidate for the various applications we are dealing with. The left- and right-facing wave's speeds are readily obtained, following Davis (1988) estimates:

$$S_R = \max\left(u_L + c_L, u_R + c_R\right),$$

$$S_L = \min\left(u_L - c_L, u_R - c_R\right),$$

where the frozen sound speed still obeys to the relation: $c^2 = \sum_k Y_k c_k^2$.

The intermediate wave speed is estimated under HLL approximation,

$$S_M = \frac{\left(\rho u^2 + p\right)_L - \left(\rho u^2 + p\right)_R - S_L (\rho u)_L + S_R (\rho u)_R}{(\rho u)_L - (\rho u)_R - S_L \rho_L + S_R \rho_R},$$

with the mixture density and mixture pressure defined previously.

From these wave speeds, the following variable states are determined,

$$\left(\alpha_k \rho_k\right)_R^* = \left(\alpha_k \rho_k\right)_R \frac{S_R - u_R}{S_R - S_M},$$

$$\left(\alpha_k \rho_k\right)_L^* = \left(\alpha_k \rho_k\right)_L \frac{S_L - u_L}{S_L - S_M},$$

$$p^* = p_R + \rho_R u_R \left(u_R - S_R\right) - \rho_R^* S_M \left(S_M - S_R\right),$$

with $\rho_R^* = \sum_k \left(\alpha_k \rho_k\right)_R^*$, and,

$$E_R^* = \frac{\rho_R E_R (u_R - S_R) + p_R u_R - p^* S_M}{\rho_R^* (S_M - S_R)},$$

$$E_L^* = \frac{\rho_L E_L (u_L - S_L) + p_L u_L - p^* S_M}{\rho_L^* (S_M - S_L)},$$

with $E = Y_1 e_1 + Y_2 e_2 + \frac{1}{2} u^2$.

The volume fraction jump is readily obtained, as in the absence of relaxation effects the volume fraction is constant along fluid trajectories,

$$\alpha_{kR}^* = \alpha_{kR}, \qquad \alpha_{kL}^* = \alpha_{kL}.$$

As the volume fraction is constant across left- and right-facing waves, the fluid density is determined from the preceding relations:

$$\rho_{kR,L}^* = \rho_{kR,L} \frac{u_{R,L} - S_{R,L}}{S_M - S_{R,L}}.$$

Internal energy jumps are determined with the help of approximate Hugoniot relations for System (4.1). Let us consider the example of fluids governed by the stiffened gas EOS (3.2). With the help of the EOS, the phasic pressures are constrained along their Hugoniot curves as functions only of the corresponding phase density,

$$p_k^*(\rho_k^*) = \left(p_k + p_{\infty k}\right) \frac{(\gamma_k - 1)\rho_k - (\gamma_k + 1)\rho_k^*}{(\gamma_k - 1)\rho_k^* - (\gamma_k + 1)\rho_k} - p_{\infty k}.$$

The phase's internal energies are then determined from the EOS: $e_{kR}^* = e_{kR}^*(p_k^*, \rho_k^*)$.

Equipped with this solver, the next step is to develop a Godunov type scheme.

Godunov type method

In the absence of relaxation terms, the conservative part of System (4.1) is updated with the conventional Godunov scheme:

$$U_i^{n+1} = U_i^n - \frac{\Delta t}{\Delta x}\left(F^*(U_i^n, U_{i+1}^n) - F^*(U_{i-1}^n, U_i^n)\right),$$

with $U = \left((\alpha\rho)_k, \rho u, \rho E\right)^T$ and $F = \left((\alpha\rho)_k u, \left(\rho u^2 + (\alpha_1 p_1 + \alpha_2 p_2)\right), \left(\rho E + (\alpha_1 p_1 + \alpha_2 p_2)\right) u\right)^T$.

The volume fraction equation is updated with the Godunov method for advection equations:

$$\alpha_{ki}^{n+1} = \alpha_{ki}^{n} - \frac{\Delta t}{\Delta x}\left((u\alpha_k)_{i+1/2}^* - (u\alpha_k)_{i-1/2}^* - \alpha_{ki,I}^{n}(u_{i+1/2}^* - u_{i-1/2}^*)\right) .$$

This scheme guarantees volume fraction positivity during the hyperbolic step. Regarding the non-conservative energy equations, there is no hope to determine accurate numerical approximation in the presence of shocks (Hou and Le Floch, 1990). Therefore, we use the simplest approximation of the corresponding equations by assuming the product $(\alpha p)_{k,i}^{n}$ constant during the time step:

$$(\alpha\rho e)_{k,i}^{n+1} = (\alpha\rho e)_{k,i}^{n} - \frac{\Delta t}{\Delta x}\left((\alpha\rho e u)_{k,i+1/2}^{*} - (\alpha\rho e u)_{k,i-1/2}^{*} + (\alpha p)_{k,i}^{n}\left(u_{i+1/2}^* - u_{i-1/2}^*\right)\right)$$

The lack of accuracy in the internal energy computation resulting from the present scheme is not so crucial. The internal energies will be used only to estimate the phase's pressure at the end of the hyperbolic step, before the relaxation one. The relaxation step will give a first correction to the internal energies, in agreement with the second law of thermodynamics. A second correction will be made with the help of the total mixture energy. The details of these two steps are described in the next subsections.

Relaxation step

This step is of major importance to fulfil interface conditions in non-uniform velocity and pressure flow conditions. It also forces the solution of the pressure non-equilibrium model (4.1) to converge to that of the equilibrium model (3.1). In the relaxation step the system to consider reads,

$$\frac{\partial \alpha_1}{\partial t} = \mu(p_1 - p_2),$$

$$\frac{\partial \alpha_k \rho_k}{\partial t} = 0,$$

$$\frac{\partial \alpha_k \rho_k e_k}{\partial t} = -p_I \mu(p_1 - p_2),$$

$$\frac{\partial \rho u}{\partial t} = 0,$$

$$\frac{\partial \rho E}{\partial t} = 0,$$

in the limit $\mu \to +\infty$.

After some manipulations the internal energy equations become:

$$\frac{\partial e_k}{\partial t} + p_I \frac{\partial v_k}{\partial t} = 0.$$

This system can be written in integral form as,

$$e_k - e_k^0 + \hat{p}_{Ik}(v_k - v_k^0) = 0,$$

with $\hat{p}_{Ik} = \dfrac{1}{v_k - v_k^0} \int_0^{\Delta t} p_I \dfrac{\partial v_k}{\partial t} dt$.

Determination of pressure averages $\hat{p}_{Ik}$ has to be done in agreement with thermodynamic considerations.

By summing the internal energy equations we have:

$$\sum_k \left(Y_k e_k - Y_k e_k^0 \right) + \sum_k \hat{p}_{Ik} (Y_k v_k - Y_k v_k^0) = 0 \ .$$

As the system conserves energy, $\sum_k \left(Y_k e_k - Y_k e_k^0 \right) = 0$.

On the other hand, mass conservation implies, $\sum_k (Y_k v_k - Y_k v_k^0) = 0$.

Therefore, the identity,

$$\sum_k \left(Y_k e_k - Y_k e_k^0 \right) + \sum_k \hat{p}_{Ik} (Y_k v_k - Y_k v_k^0) = 0 ,$$

is fulfilled if the various pressure averages are taken equal, i.e.,

$\hat{p}_{Ik} = \hat{p}_I = p$.

This pressure average estimate also agrees with the entropy inequality.

The system to solve is thus composed of equations,

$$e_k(p\ , v_k) - e_k^0(p_k^0, v_k^0) + \hat{p}_I (v_k - v_k^0) = 0 , \ k = 1, N , \tag{4.4}$$

which involves 2+1 unknowns, $v_k \, (k = 1, 2)$ and p . Its closure is achieved by the saturation constraint,

$$\sum_k \alpha_k = 1 ,$$

that is rewritten under the form,

$$\sum_k (\alpha\rho)_k \, v_k(p) = 1 \ . \tag{4.5}$$

As the $(\alpha\rho)_k$ are constant during the relaxation process, this system can be replaced by a single equation with a single unknown (p). With the help of the EOS (4.3) the energy equations become,

$$v_k(p\ ) = v_k^0 \frac{p_k^0 + \gamma_k p_{\infty k} + (\gamma_k - 1)\hat{p}_I}{p\ + \gamma_k p_{\infty k} + (\gamma_k - 1)\hat{p}_I} \ ,$$

and thus the only equation to solve (for p) is (4.5).

Once the relaxed pressure is found, the phase's specific volumes and volume fractions are determined.

However, there is no guarantee that the mixture EOS or the mixture energy be in agreement with this relaxed pressure. In order to respect total energy and correct shock dynamics on both sides of the interface, the following correction is employed.

Reset step

As the volume fractions have been estimated previously by the relaxation method, the mixture pressure can be determined from the mixture EOS based on the mixture energy which is known from the solution of the total energy equation. As the mixture total energy obeys a conservation law, its evolution is accurate in the entire flow field and in particular at shocks.

Again considering fluids governed by the stiffened gas EOS, the mixture EOS is given by (3.3). This EOS is valid in pure fluids and in the diffuse interface zone. As it is valid in pure fluids and based on the total energy equation, it guarantees correct wave dynamics on both sides of the interface. Inside the

numerical diffusion zone of the interface, numerical experiments show that the method is accurate too, as the volume fractions used in the mixture EOS have a quite accurate prediction from the relaxation step.

Once the mixture pressure is determined the internal energies of the phases are reset with the help of their respective EOS before going to the next time step,

$$e_k = e_k(p, \alpha_k \rho_k, \alpha_k) \ . \tag{4.6}$$

Shock propagation in multiphase mixtures

When the flow involves material interface only, the preceding algorithm is particularly simple and efficient. But in some situations, mixtures of materials are present, eventually in the presence of shocks. This occurs for example in the study of detonation waves in heterogeneous materials. In this situation, the shock energy has to be apportioned correctly among the phases; otherwise the shock speeds as well as the various jumps are incorrect. The goal is thus to impose the shock conditions (3.4) in the pressure equilibrium solution. This issue has been addressed in Petitpas et al. (2007) and a solution method was given in Petitpas et al. (2009). It consists in replacing Eq. (4.4) in the previous pressure relaxation step by,

$$e_k(p\ , v_k) - e_k^0(p_k^0, v_k^0) + \frac{p + p_0}{2}(v_k - v_k^0) = 0\ ,\ k = 1, N\ , \tag{4.7}$$

where the state with superscript 0 indicates the Hugoniot pole. This state has to be constant inside the shock layer. To do this, additional evolution equations are used to replace the internal energy equations of System (4.1), in the shock layer only. These equations read:

$$\frac{\partial v_k^0}{\partial t} + u \frac{\partial v_k^0}{\partial x} = 0\ ,\ k=1,2, \tag{4.8}$$

$$\frac{\partial p_0}{\partial t} + u \frac{\partial p_0}{\partial x} = 0\ .$$

Thanks to (4.7) and (4.8) the method converges to the correct shock state.

Summary of the numerical method

The numerical method can be summarized as follows:

- At each cell boundary solve the Riemann problem of System (4.1) in the absence of relaxation terms with the HLLC solver.

- Evolve all flow variables with the Godunov type method.

- Determine the relaxed pressure and especially the volume fraction by solving Equation (4.5) with the help of the Newton method. Equations (4.4) are used if interfaces separate pure fluids. If one of the media corresponds to a multiphase mixture, Equations (4.4) are replaced by (4.7). In this instance, (4.8) have to be solved in the shock layer. The shock layer is detected thanks to shock indicators such as Toro (1997) (see paragraph 14.6.4) or Menikoff and Shaw (2010).

- Compute the mixture pressure with Equation (3.3).

- Reset the internal energies with the computed pressure with the help of their respective EOS (4.6).

- Go to the first item for the next time step.

Computational example

A non-conventional computational example is shown in the Figure 2. A piston impacts a liquid column with a curved liquid-gas interface. A Richtmyer-Meshkov type instability appears, as expected. Unexpected features appear too, as cavitation pockets are created in the liquid domain, due to liquid jet

presence. To deal with such a flow, the model has to deal with material interfaces, shocks and expansions waves. It must also predict dynamic interfaces appearance. Cavitation pockets are here consequences of the small amount of gas present in the liquid that grows under expansion effects as a result of the pressure equilibrium condition.

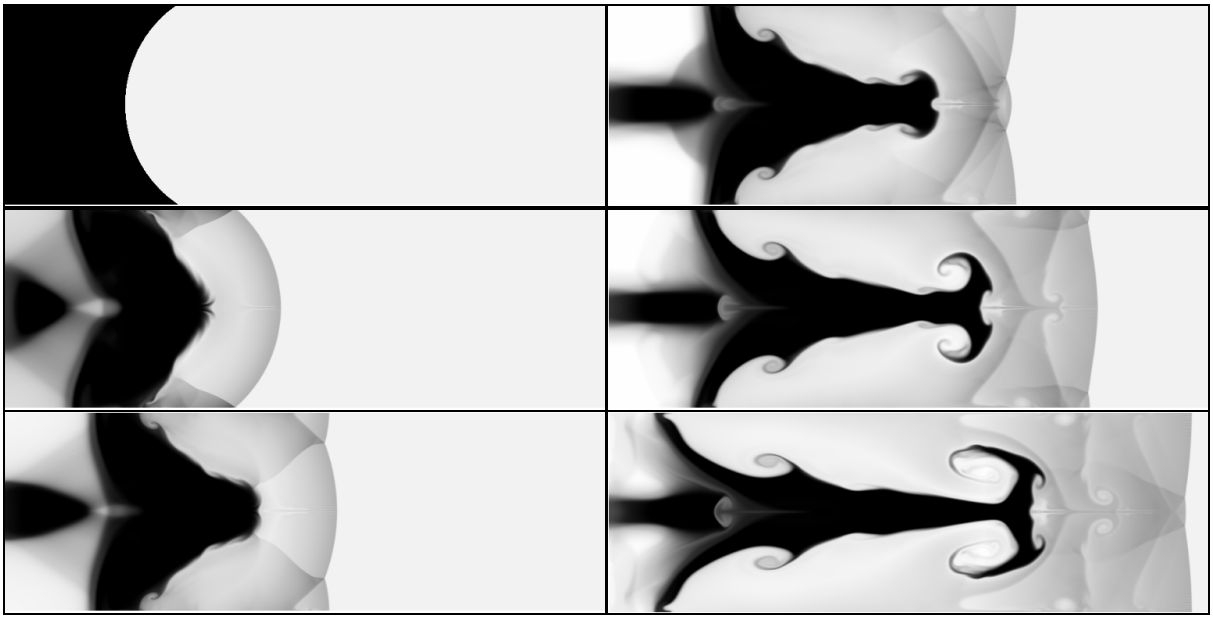

Figure 2 –Richmyer-Meshkov instability with a cavitating liquid and a non miscible gas.

On the basis of the Kapila et al. (2001) model, several extensions have been done. Some of them are summarized in the rest of the paper.

5 Capillary effects

The following capillary flow model is a slight variation of the Perigaud and Saurel (2005) model where the CSF method of Brackbill et al. (1992) has been embedded in the compressible Kapila model. The corresponding system reads:

$$
\begin{aligned}
&\frac{\partial \alpha_1}{\partial t} && + \vec{u}.\vec{\nabla}\alpha_1 - \frac{(\rho_2 c_2^2 - \rho_1 c_1^2)}{\frac{\rho_1 c_1^2}{\alpha_1} + \frac{\rho_2 c_2^2}{\alpha_2}} \operatorname{div}(\vec{u}) && = 0 \\
&\frac{\partial \rho Y_1}{\partial t} && + \operatorname{div}(\rho Y_1 \vec{u}) && = 0 \\
&\frac{\partial \rho}{\partial t} && + \operatorname{div}(\rho \vec{u}) && = 0 \\
&\frac{\partial \rho \vec{u}}{\partial t} && + \operatorname{div}\left(P\bar{\bar{I}} + \rho \vec{u} \otimes \vec{u} - \sigma\left(\left|\vec{\nabla} Y_1\right| \bar{\bar{I}} - \frac{\vec{\nabla} Y_1 \otimes \vec{\nabla} Y_1}{\left|\vec{\nabla} Y_1\right|} \right) \right) && = 0 \\
&\frac{\partial \rho (e + \frac{\sigma\left|\vec{\nabla} Y_1\right|}{\rho} + \frac{1}{2}\vec{u}^2)}{\partial t} && + \operatorname{div}\left((\rho(e + \frac{\sigma\left|\vec{\nabla} Y_1\right|}{\rho} + \frac{1}{2}\vec{u}^2) + P)\vec{u} - \sigma\left(\left|\vec{\nabla} Y_1\right| \bar{\bar{I}} - \frac{\vec{\nabla} Y_1 \otimes \vec{\nabla} Y_1}{\left|\vec{\nabla} Y_1\right|} \right).\vec{u} \right) && = 0
\end{aligned}
\qquad (5.1)
$$

This formulation presents at least two advantages:

- Compressible effects are present in conjunction to surface tension ones.

- There is no interface width, compared to the Cahn and Hilliard (1958) second gradient theory that needs too fine resolution for practical applications.

A computation example and comparison with experiments is shown in the Figure 3.

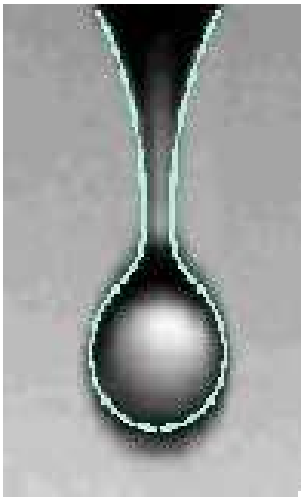

Figure 3: Comparison of computed drop formation under gravity effects (light lines) versus experimental photograph (grey contours). System (5.1) is solved everywhere, in pure liquid, pure gas and at the interface.

6 Phase transition

This extension has been done in Saurel et al. (2008) on the basis of system's entropy production examination. In the absence of capillary effects, the resulting system reads,

$$\frac{\partial \alpha_1}{\partial t} + \vec{u}.\mathrm{grad}(\alpha_1) = \frac{(\rho_2 c_2^2 - \rho_1 c_1^2)}{\frac{\rho_1 c_1^2}{\alpha_1} + \frac{\rho_2 c_2^2}{\alpha_2}} \mathrm{div}(\vec{u}) + \rho\nu(g_2 - g_1) \frac{\frac{c_1^2}{\alpha_1} + \frac{c_2^2}{\alpha_2}}{\frac{\rho_1 c_1^2}{\alpha_1} + \frac{\rho_2 c_2^2}{\alpha_2}} + H(T_2 - T_1) \frac{\frac{\Gamma_1}{\alpha_1} + \frac{\Gamma_2}{\alpha_2}}{\frac{\rho_1 c_1^2}{\alpha_1} + \frac{\rho_2 c_2^2}{\alpha_2}},$$

$$\frac{\partial \alpha_1 \rho_1}{\partial t} + \mathrm{div}\left(\alpha_1 \rho_1 \vec{u}\right) = \rho\nu\left(g_2 - g_1\right),$$

$$\frac{\partial \alpha_2 \rho_2}{\partial t} + \mathrm{div}\left(\alpha_2 \rho_2 \vec{u}\right) = -\rho\nu\left(g_2 - g_1\right), \qquad (6.1)$$

$$\frac{\partial \rho \vec{u}}{\partial t} + \mathrm{div}\left(\rho \vec{u} \otimes \vec{u}\right) + \mathrm{grad}(p) = 0,$$

$$\frac{\partial \rho E}{\partial t} + \mathrm{div}\left(\left(\rho E + p\right)\vec{u}\right) = 0,$$

with the following notations,

$g_k = h_k - T_k s_k$ represents the Gibbs free energy,

H represents the temperature relaxation parameter, and

ν is the mass transfer kinetic parameter.

Some comments are due regarding the volume fraction equation. The first term in the right hand side, present in the Kapila et al. (2001) model, represents mechanical relaxation effects, present in all zones where the velocity divergence is non zero (shocks, compressions, expansions). The second term represents volume variations due to mass transfer, in a context where both phases are compressible. The last group of terms represents dilatation effects due to heat transfer. Γ_k represents the Grüneisen coefficient of the phase k.

The model needs thermodynamic parameters on one hand and kinetics ones, such as H and ν on the other hand. In the present formulation, each fluid has its own thermodynamics and the equation of state parameters are determined on the basis of the phase diagram, as detailed in Le Metayer et al. (2004). Regarding kinetic parameters, we have learnt in the beginning of this presentation that it was

possible to fulfil interface condition of simple contact by using infinite mechanical relaxation parameters. Here, infinite thermal and mass transfer kinetics are used (infinite H and ν). It means that locally thermodynamic equilibrium is assumed. This renders possible the consideration of phase transition fronts propagating at global finite rate (Saurel et al., 2008).

Infinite heat and mass transfer kinetic parameters have been used on the example shown in the Figure 4 at liquid-vapour interfaces when the liquid is overheated (metastable). At vapour-non condensable gas interfaces, the same kinetic parameters have been set to zero, in order to fulfil contact interface conditions.

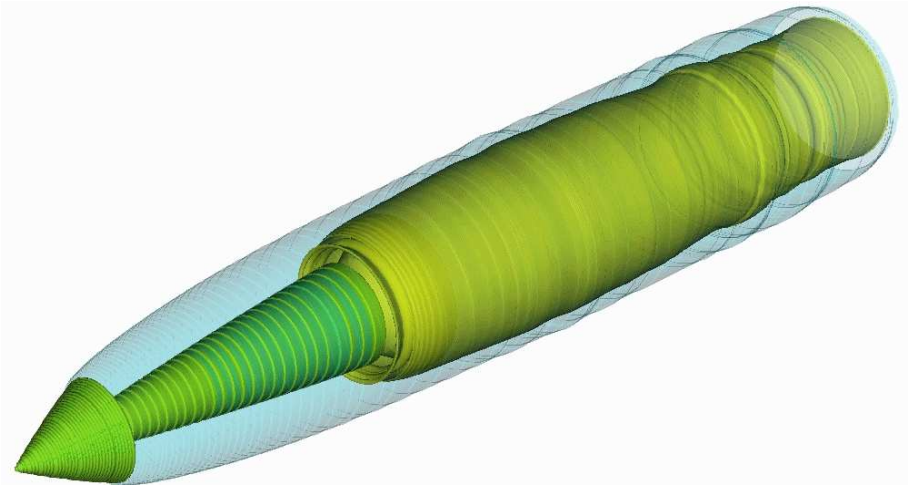

Figure 4: Cavitating flow around a hypervelocity underwater missile. Combustion gases are shown in yellow contours and are in contact with vapour, in blue colour. The vapour is separated from the liquid (not shown) by an evaporating interface. Two different types of interfaces are thus present in this example. The results are issued of Petitpas et al. (2009).

7 Detonations

To deal with the detonation of condensed energetic materials, possibly heterogeneous, the same flow model as previously can be used except regarding the equations of state that must contain appropriate reference energy yielding exothermic heat of reaction. For example, the stiffened gas equation of state (3.2) now expresses as,

$$p_k = (\gamma_k - 1)\rho_k(e_k - q_k) - \gamma_k p_{\infty k},$$

where q_k represents the reference energy.

It is then necessary to use finite rate heat and mass transfer coefficients, respectively H and ν. Let us present first an illustrative example. A detonation tube is filled with a heterogeneous explosive mixture. A shock wave is emitted by a detonator and transforms to a detonation that propagates in the explosive, loaded with aluminium particles.

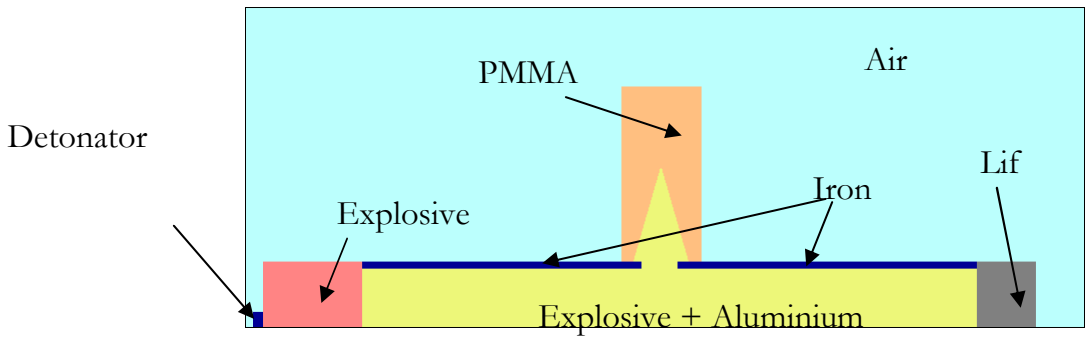

Material interfaces are present too as 5 different materials have to be considered. As previously mentioned, the same equations are solved everywhere with the same flow solver. The results

shown in the Figure 5 are taken from Petitpas et al. (2009).

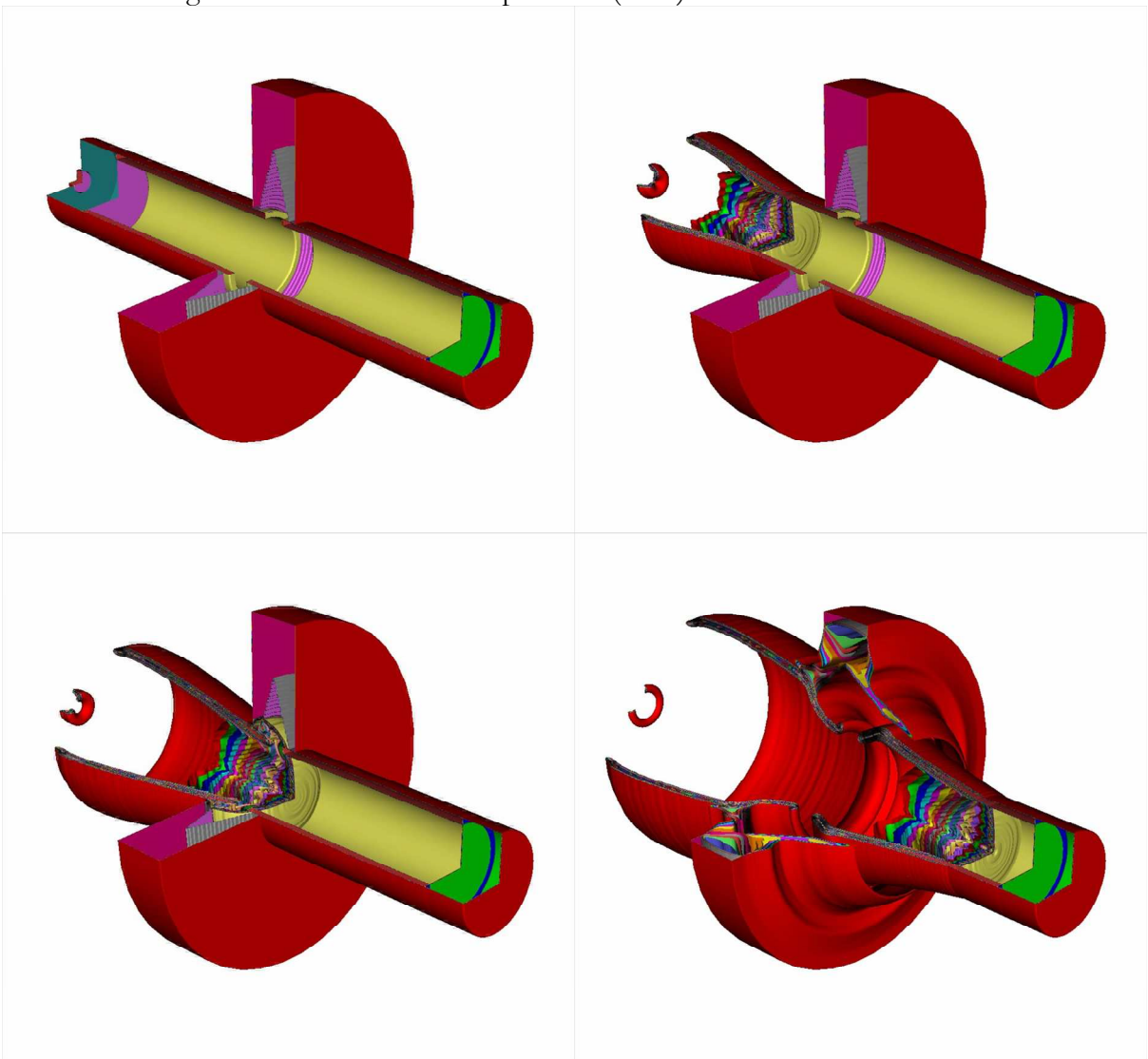

Figure 5: Mixture density contours at the initial time and at three successive times showing detonation dynamics and interfaces motion.

Starting from the flow model expressed in Section 6, it is possible to determine generalized Chapman Jouguet relations, yielding non-ideal detonation behaviour even in pure 1D plannar flow configuration. Indeed, expressing the flow model between the shock front and the sonic surface, in the detonation wave frame of reference, the following expression for the velocity divergence is obtained:

$$\frac{d\bar{u}}{dx}=\frac{1}{\rho(c^2-\bar{u}^2)}\left(\frac{\Gamma_1}{\alpha_1}\frac{\Gamma_2}{\alpha_2}\frac{\left(\frac{\rho_2c_2^2}{\Gamma_2}-\frac{\rho_1c_1^2}{\Gamma_1}\right)}{\left(\frac{\rho_1c_1^2}{\alpha_1}+\frac{\rho_2c_2^2}{\alpha_2}\right)}H(T_2-T_1)+\left(\frac{\left(\frac{\rho_2c_2^2}{\Gamma_2}-\frac{\rho_1c_1^2}{\Gamma_1}\right)}{\left(\frac{\rho_1c_1^2}{\alpha_1}+\frac{\rho_2c_2^2}{\alpha_2}\right)}\left(\frac{c_1^2}{\alpha_1}+\frac{c_2^2}{\alpha_2}\right)+h_2-\frac{c_2^2}{\Gamma_2}-\left(h_1-\frac{c_1^2}{\Gamma_1}\right)\right)\frac{\dot{m}_1}{\left(\frac{\alpha_1}{\Gamma_1}+\frac{\alpha_2}{\Gamma_2}\right)}\right)$$

The generalized Chapman Jouguet relation appears immediately. On the sonic surface characterized by, $\bar{u}=c$,
necessarily,

$$\frac{\Gamma_1}{\alpha_1}\frac{\Gamma_2}{\alpha_2}\frac{\left(\frac{\rho_2c_2^2}{\Gamma_2}-\frac{\rho_1c_1^2}{\Gamma_1}\right)}{\left(\frac{\rho_1c_1^2}{\alpha_1}+\frac{\rho_2c_2^2}{\alpha_2}\right)}H(T_2-T_1)+\left(\frac{\left(\frac{\rho_2c_2^2}{\Gamma_2}-\frac{\rho_1c_1^2}{\Gamma_1}\right)}{\left(\frac{\rho_1c_1^2}{\alpha_1}+\frac{\rho_2c_2^2}{\alpha_2}\right)}\left(\frac{c_1^2}{\alpha_1}+\frac{c_2^2}{\alpha_2}\right)+h_2-\frac{c_2^2}{\Gamma_2}-\left(h_1-\frac{c_1^2}{\Gamma_1}\right)\right)\frac{\dot{m}_1}{\left(\frac{\alpha_1}{\Gamma_1}+\frac{\alpha_2}{\Gamma_2}\right)}=0.$$

Thus, when heat transfers are absent the conventional CJ relation is recovered: $\dot{m}_1=0$ when $\bar{u}=c$.

These extended CJ relations have non trivial consequences. While the CJ detonation velocity is considered as the maximum admissible detonation speed, heterogeneous explosives can overpass this

limit. This theoretical fact has been checked by Baudin et al. (2010) on the basis of experiments done at Sarov in Russia, with the help of various liquid explosive mixtures loaded with inert solid particles. The heat transfers are not responsible for the increase in detonation velocity. The explanation comes from the fact that, in temperature non-equilibrium conditions the phases have unconstrained dilatation. Indeed, due to the fast phenomenon occurring in the reaction zone and due to the quite large particle sizes, thermal equilibrium assumed in conventional CJ and ZND models is not justified and yields to underestimated detonation speeds, as a consequence of constrained dilatation of the various substances.
The present flow model, CJ conditions and ZND structure have been recently investigated in details by Schoch et al. (2012) for the study of highly non-ideal ammonium nitrate explosives, showing in particular impressive comparison with experimental detonation records in a broad range of confinements and wide range of charge diameters.

8 Perspectives

Diffuse interface methods are now mature enough to deal with realistic and advanced applications. There are however many fundamental issues to address:

- The shock relations (3.2) have been demonstrated for weak shocks. They have been compared to experimental data for strong shocks (in the megabar range) showing excellent agreement too (Saurel et al., 2007). However, there is no mathematical proof of their validity for strong shocks.
- The numerical method summarized in Section 4 and its variants (Pelanti and Shyue, 2012) are very efficient for high speed flows. However, many applications deal with low Mach number flow conditions and there is a clear need for efficient algorithms at all Mach number for diffuse interface models. Efforts in this direction have been done by Le Martelot et al. (2012).
- Another numerical issue deals with long time evolutions, where interfaces become too smeared with upwind scheme computations. There is thus a clear need to sharpen interfaces without losing conservation properties.
- There are also extra mathematical modelling issues when dealing with extra physics extensions, such as for example, hot spot modelling in shock to detonation transition in the area of combustion, solid fluid coupling (Favrie et al., 2009) to make a bridge between fluid and solid mechanics, the direct numerical simulation of boiling flows in the area of energetics.
- Another important modelling issue is related to velocity drift effects restoration in diffuse interface formulations. Attempts in this direction have been done by Guillard and Duval (2007), Saurel et al. (2010), Saurel et al. (2012).

Acknowledgements. The first author is particular grateful to Stéphane Gerbi and Christophe Bourdarias for their kind invitation at the AMIS 2012 conference in Chambery.

References

Abgrall R. and Saurel R., Discrete equations for physical and numerical multiphase mixtures. Journal of Computational Physics, 186 (2), 361-396, 2003

Baer, M.R. and Nunziato, J.W., (1986) A two-phase mixture theory for the deflagration-to-detonation transition (DDT) in reactive granular materials. Int. J. of Multiphase Flow, vol. 12 (6), 861

Benson, D.J. (1992) Computational methods in Lagrangian and Eulerian hydrocodes. Computer Methods in Applied Mechanics and Engineering, vol. 99, pp. 235-394

Brackbill J., Kothe D. and Zemach C., A continuum method for modelling surface tension. Journal of Computational Physics, 100, 335-354, 1992

Cahn J. and Hilliard J., Free energy of a nonuniform system. Part I: Interfacial free energy. Journal of Chemical Physics, 28, 258, 1958

Chinnayya, A., Daniel, E. and Saurel, R. (2004) Computation of detonation waves in heterogeneous energetic materials. Journal of Computational Physics, vol. 196, pp. 490-538

Davis, S.F. (1988) Simplified second order Godunov type methods. SIAM J. Sci. Stat. Comput., 9: 445-473

Farhat, C. and Roux, F.X. (1991) A method for finite element tearing and interconnecting and its parallel solution algorithm. International Journal for Numerical Methods in Engineering, vol. 32,pp. 1205-1227

Favrie N., Gavrilyuk S. and Saurel R., Solid-fluid diffuse interface model in cases of extreme deformations. Journal of Computational Physics, 228, 6037-6077, 2009

Fedkiw, R., Aslam, T., Merriman, B. and Osher, S. (1999) A Non-oscillatory Eulerian Approach to Interfaces in Multimaterial Flows (the Ghost Fluid Method). Journal of Computational Physics 152(2) , pp 457-492

Gavrilyuk, S. and Saurel, R. (2002) A compressible multiphase flow model with microinertia . Journal of Computational Physics, 175, pp 326-360

Glimm, J., Grove, J.W., Li, X.L., Shyue, K.M., Zhang, Q. and Zeng, Y. (1998) Three dimensional front tracking. SIAM J. Scientific Computing, vol.19, pp. 703-727

Godunov, S. K. (1959) A Difference scheme for numerical solution of discontinuous solution of hydrodynamic equations. Math. Sbornik, 47, 271–306

Gueyffier, D., Li, L., Nadim, A., Scardovelli, R. and Zaleski, S. (1999) Volume-Of-Fluid Interface Tracking with Smoothed Surface Stress Methods for Three-Dimensional Flows. Journal of Computational Physics, vol. 152 , pp. 423-456

Guillard, H. and Duval, F. (2007) A Darcy law for the drift velocity in a two-phase flow model. J. Comp. Phys. 224, 288–313

Hirt, C.W. and Nichols, B.D. (1981) Volume Of Fluid (VOF) method for the dynamics of free boundaries. Journal of Computational Physics, vol.39, pp. 201-255

Hirt, C.W., Amsden, A.A., and Cook , J.L. (1974) An Arbitrary Lagrangian Eulerian Computing Method for all flow Speeds. Journal of Computational Physics, vol.135, pp. 203-216

Hou, T. and Le Floch, P. (1994) Why non-conservative schemes converge to wrong solutions: Error analysis. Mathematics of Computations 62(206), 497-530

Kapila, A.K., Menikoff, Bdzil, J.B., Son, S.F. and Stewart, D.S. (2001) Two-phase modeling of deflagration to detonation transition in granular materials: Reduced equations. Phys. Fluids 13(10), 3002-3024

Karni, S. (1994) Multicomponent flow calculations by a consistent primitive algorithm. J. Comp. Phys. 112, 31-43

Le Martelot, S., Nkonga, B. and Saurel, R. (2012) Liquid and liquid-gas flows at all speeds: Reference solutions and numerical schemes. Journal of Computational Physics, submitted

Le Metayer, O., Massoni, J. and Saurel, R. (2004) Elaboration des lois d'état d'un liquide et de sa vapeur pour les modèles d'écoulements diphasiques. Int. J. of Thermal Sciences 43, 265-276 (in French)

LeVeque, R.J. and Keh-Ming Shyue (1996) Two-Dimensional Front Tracking Based on High Resolution Wave Propagation Methods. Journal of Computational Physics 123 (2), pp 354-368

Menikoff, R. and Shaw, M.S., 2010. Reactive Burn models and ignition & growth concept, Los Alamos National Laboratory Report, LA-UR-10-01870

Miller, G.H. and Puckett, E.G. (1996) A High-Order Godunov Method for Multiple Condensed Phases. Journal of Computational Physics 128(1), pp 134-164

Mulder, W., Osher, S. and Sethian, J.A. (1992) Computing interface motion: The compressible Rayleigh-Taylor and Kelvin-Helmholtz instabilities. Journal of Computational Physics, vol.100, p. 209

Osher, S. and Fedkiw, R. (2001) Level Set Methods: An overview and some recent results. Journal of Computational Physics, vol. 169, pp. 463-502

Pelanti, M. and Shyue, K.M. (2012) A mixture energy consistent 6-equation two-phase model for fluids with interfaces and cavitation phenomena. Conference Applied Math. In Savoie (AMIS 2012), 19-22 june 2012, Chambery, France

Perigaud G. and Saurel R., A compressible flow model with capillary effects, Journal of Computational Physics, 209, 139-178, 2005

Petitpas, F., Franquet, E., Saurel, R. and Le Metayer, O. (2007) A relaxation-projection method for compressible flows. Part II : Artificial heat exchanges for multiphase shocks. Journal of Computational Physics 225(2), 2214-2248

Petitpas F., Saurel R., Franquet E. and Chinnayya A., Modelling detonation waves in condensed

energetic materials: Multiphase CJ conditions and multidimensional computations. Shock Waves, 19(5), 377-401, 2009

Petitpas, F., Massoni, J., Saurel, R., Lapebie, E. and Munier, L. (2009) Diffuse interface model for high speed cavitating underwater systems. Int. J. Multiphase Flow 35, 747-759

Saurel R. and Abgrall R., A multiphase Godunov method for compressible multifluid and multiphase flows. Journal of Computational Physics, 150, 425-467, 1999

Saurel, R. and Le Metayer, O. (2001) A multiphase model for interfaces, shocks, detonation waves and cavitation. Journal of Fluid Mechanics, Vol. 431, pp 239 – 271

Saurel R., Gavrilyuk S. and Renaud F., A multiphase model with internal degrees of freedom: Application to shock-bubble interaction. Journal of Fluid Mechanics, 495, 283-321, 2003

Saurel R., Le Metayer O., Massoni J., and Gavrilyuk S., Shock jump relations for multiphase mixtures with stiff mechanical relaxation . Shock Waves, 16 (3), 209-232, 2007

Saurel R., Petitpas F. and Abgrall R., Modelling phase transition in metastable liquids. Application to cavitating and flashing flows. Journal of Fluid Mechanics, 607, 313-350, 2008

Saurel R., Favrie N., Petitpas F., Lallemand M.H. and Gavrilyuk S., Modelling irreversible dynamic compaction of powders. Journal of Fluid Mechanics, 664, 348-396, 2010.

Saurel R., Petitpas F. and Berry R.A., Simple and efficient relaxation methods for interfaces separating compressible fluids, cavitating flows and shocks in multiphase mixtures. Journal of Computational Physics, 228, 1678-1712, 2009.

Saurel, R., Favrie, N., Petitpas, F., Lallemand, M.H. and Gavrilyuk, S. (2010) Modelling irreversible dynamic compaction of powders. J. Fluid Mech. 664, 348-396

Saurel, R., Huber, G., Jourdan, G., Lapebie, E. and Munier, L. (2012) Modelling spherical explosions with turbulent mixing and post-combustion. Physics of Fluids, submitted

Schoch, S., Nikiforakis, N., Lee, B.J. and Saurel, R. (2012) Multi-phase simulation of ammonium nitrate emulsion detonation. Combustion and Flame, submitted

Sethian, J. (2001) Evolution, Implementation and Application of Level Set and Fast Marching Methods for Advancing Fronts. Journal of Computational Physics, vol. 169, pp. 503-555

Scheffer, D.R. and Zukas, J.A. (2000) Practical aspects of numerical simulation of dynamic events: material interfaces. International Journal of Impact Engineering, vol. 24, n° 5-6, pp. 821-842

Toro, E.F., Spruce, M. and Speares, W. (1994) Restoration of the contact surface in the HLL Riemann solver. Shock Waves, 4, pp 25-34

Toro, E.F. (1997) Riemann Solvers and Numerical Methods for Fluid Dynamics, Springer, Berlin

Von Neumann, J. and Richtmyer, R. D. (1950). A method for the numerical calculation of hydrodynamic shocks. Journal of Applied Physics 21(3), 232–237

Wood, A.B. (1930) A textbook of sound. Bell Eds.